

DYNAMIC ANALYSIS OF A RUMOR PROPAGATION MODEL

Rui Ma¹, Zhuanting Ma², Baojun Yang³

Rumor propagation rapidly and can cause significant damage. Based on the premise of a rumor management mechanism, this study analyzes the propagation rules among latent disseminators, disseminators, and non-disseminators. We have crafted a rumor propagation model and have established the presence of an equilibrium state within it. Additionally, we have analyzed the local and global stability of this equilibrium, as well as determined the model's propagation threshold. By determining the equilibrium point of the model, we examine the link between this issue and the crisis's progression pattern, and derive the threshold R_0 . The propagation-free equilibrium is stable within a certain range when $R_0 < 1$, and propagation exhibits a downward trend until it ultimately subsides. Subsequently, the factors affecting the threshold R_0 are investigated through numerical experiments. Finally, the influence of these factors on the development trend of rumor is analyzed in detail. This research can help authorities understand the principles of propagation and offer guidance.

Keywords: Equilibrium points; Rumor; Stability; Threshold

MSC2020: 53C05.

1. Introduction

The protests over the Israel-Gaza conflict [1, 2, 3] have not only garnered attention on campus but have also sparked political debate. President Biden has condemned extremism on both sides, while former President Trump has blamed the Biden administration for sending the wrong signals. Additionally, some congressional members have proposed more radical measures, such as deploying the National Guard to university campuses to protect Jewish Americans, as suggested by Missouri Republican Senator Josh Hawley. These protests not only raise concerns about campus safety [2] but also touch on broader issues such as freedom of speech and the politicization of campuses. While lawmakers struggle to balance these competing interests, calls for accountability are growing. Some have suggested that students involved in the protests should be expelled from campus, or university funding should be suspended [4].

The policies implemented by the United States in the latest Palestinian-Israeli conflict have triggered widespread societal debates and discontent, these sudden public crisis events will lead to different degrees of rumor crisis, which makes the official face increasing pressure. After the outbreak of such incidents, all kinds of information propagation rapidly through

¹School of Management, North Minzu University, Wenchang Street, Yinchuan, 750021, Ningxia, China.
e-mail: maruionly@163.com

²School of Mathematics and Information Science, North Minzu University, Wenchang Street, Yinchuan, 750021, Ningxia, China. e-mail: 19996255521@163.com

³School of Business, North Minzu University, Wenchang Street, Yinchuan, 750021, Ningxia, China .
e-mail: bmdybj@sina.com

the Internet, and the malicious promotion of we-media platforms makes the rumor of public opinion emergencies further evolve and the prevention. At this time, if the official fail to make use of the effective opportunity of rumor governance, it will lead to the further vicious evolution of rumor, which will eventually seriously threaten social stability and social and economic development [2, 4].

The complex propagation environment has led to a chaotic and unpredictable rumor, which is difficult to manage [5, 6, 7]. The convenient propagation of rumor and the rapid propagation of views are often used by lawbreakers to interfere with the rumor environment. For sensitive social events, lawbreakers may release misinformation or extreme views, leading to confusion in the direction of rumor, intensification of social contradictions, and even mass incidents such as Anti-war protests at universities across the United States, which may hinder social stability and official work [8].

Grasping the diffusion process of rumor is helpful to take targeted measures when managing the rumor [9]. At present, most of the models studying rumor propagation mechanism are derived from classical infectious disease SIS models [10, 11, 12] or SIR models [13]. However, due to the complexity of the online environment and the aspects of rapid propagation, in actual rumor events, the population participating in the event will increase rapidly and the mobility is very strong. At the same time, the authority's countermeasures will also have an impact on the conversion of the three groups of people. Therefore, We have established the mode should take into account the influence of population flow and authority intervention on rumor propagation.

This study divides the population in rumor environment into four categories: latent disseminators, disseminators, non-disseminators and leaver and establishes a *LDN* model [14] with rumor channelization coefficient, population inflow rate and outflow rate. In this study, we examine the propagation mechanism of rumor events within a dynamic rumor using a model-based approach. We analyze the critical elements that impact the progression of rumor events. Subsequently, we analyze the solution to the model and propose policy recommendations. This paper has been arranged as follows: In Section 2, we have formulated the model. The positivity and boundedness of solutions are discussed in Section 3. Equilibrium points and threshold of the model are given in Section 4. In Section 5, We analyzed the stability of the model. In Section 6, we validate the model with matlab and estimate the model parameters sensitivity analysis. Finally in Section 7, some conclusions are summarized.

2. Model formulation

Rumor propagation regulations can be outlined as follows:

(1) The propagation of rumor often severe and quick. Some are unalterable (For example, the leaver C) and the leaver should not reappear the state $L(t)$.

(2) The non-disseminators(N) are considered to no longer enter the early transmission phase latent disseminators (L) and susceptible to a frequented propagation issue.

(3) At the initial stage ($t = 0$), the entire populace remains oblivious to the misinformation until its propagation through the first rumor. In the transition diagram, the influx rate of the populace A is marked by users engaging with the pertinent rumor environment. Conversely, ω represents the outflow rate, signifying users who lose interest in the rumor matter and subsequently disengage from the online platform (as depicted in Figure 1).

(4) We assume that the controlling agent ("authorities") has the ability to impact the propagation of the rumor through some policies. In this study we consider the intervention of the authorities caused people to leave the environment's propagation rate is ω_1 .

(5) In numerous epidemiological frameworks, the bilinear incidence rate is frequently represented by βSI , (where S , and I indicate the quantity of susceptible individuals and infectious individuals) is frequently used (see [15, 16] and the references therein). Capasso and Serio [17] brought in the saturated incidence rate $\frac{\beta SI}{1+\alpha I}$, where $\frac{\beta I}{1+\alpha I}$ tends to a saturation level as I grow in significance. Furthermore, βI quantifies the infection force when the disease encounters a fully susceptible population, while $\frac{1}{1+\alpha I}$ captures the inhibitory influence stemming from behavioral shifts among susceptible individuals as their quantity rise or due to the congestion impact of infected individuals. This refined prevalence rate surpasses the bilinear βSI model in its realism, as it incorporates behavioral adaptations and crowding dynamics, ensuring the contact rate remains bounded through judicious parameter selection. and it was used in many epidemic models afterwards [13, 14, 15] The latent disseminators gets the propagation by direct contact alone. We consider the saturation propagation rate $f(t) = \frac{\beta \hat{L}(t) \hat{D}(t)}{1+\alpha D(t)}$, where $\alpha, \beta > 0$, and β is the rumor rate of humans easy to dissemination class, and α actions the inhibitory effect of propagating individuals[14, 15, 16]. Hence, we introduce a compartmental diagram for the rumor propagation

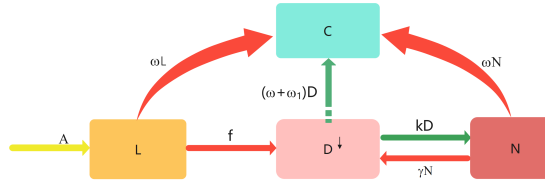


FIGURE 1. a compartmental diagram for the rumor propagation

(Fig. 1). The system (1) of differential equations plays a pivotal role in regulating population dynamics.

$$\begin{cases} \frac{dL}{dt} = A - \frac{\beta LD}{1+\alpha D} - \omega L, \\ \frac{dD}{dt} = \frac{\beta LD}{1+\alpha D} + \gamma N - (k + \omega + \omega_1)D, \\ \frac{dN}{dt} = kD - (\gamma + \omega)N, \\ \frac{dC}{dt} = \omega L + \omega N + (\omega + \omega_1)D. \end{cases} \quad (1)$$

The equivalent mathematical representation or formulation for the diffusion dynamics of rumor is as follows: γ represents the recurrence rate of rumor propagation, while k denotes the termination rate of this propagation.

The refined model exhibits that the variables L , D , and N are independent of C , indicating their autonomy from C . For in-depth analysis, it suffices to focus on the simplified system outlined below. Given that we are observing a human population, all parameters assume positive values. The initial configuration for system (1) is defined as: $L > 0$, $D \geq 0$, $N \geq 0$. We proceed to investigate system (1) within a practical domain characterized by: insert specific constraints or bounds on L , D , and N if provided, or simply state "a physically meaningful range".

$$\mathcal{U} = (L, D, N) \in \mathbb{R}_+^3 / 0 < L + D + N \leq \frac{A}{\omega}. \quad (2)$$

3. Non-negativity and boundedness of the model

In order to system (1) work, It is crucial to indicate that all the state variables maintain positivity throughout the time span, meaning that given positive initial conditions,

the solution to system (1) will persist in being positive and within a certain range for all $t > 0$.

Lemma 3.1. The symbol \mathcal{U} denotes a positively invariant area within system (1), characterized by its ability to attract all solutions to the central region of the positive quadrant.

Proof. We reformulate system (1) into a vector form for simplicity and reduced repetition $\frac{dF}{dt} = KF + g$,

$$F = \begin{bmatrix} L \\ D \\ N \end{bmatrix}, K = \begin{bmatrix} \frac{-\beta D}{1+\alpha D} - \omega \\ -(k + \omega + \omega_1) \\ -(\gamma + \omega) \end{bmatrix}, g = \begin{bmatrix} A \\ \frac{-\beta D}{1+\alpha D} + \gamma N \\ kD \end{bmatrix}, \quad (3)$$

Then, we can get

$$\frac{dF}{dt} \geq KF$$

From above, it holds the integral differential equation

$$F \geq F(0) \exp\left(\int_0^t Kdt\right) > 0. \quad (4)$$

Hence, given the initial condition $F(0) > 0$, the solutions of system (1) remain positive for all $t > 0$. In the following section of the proof, we integrate all the state variables of system (1) into one collective variable, aggregated form:

$$\begin{aligned} \frac{dM}{dt} &= \frac{dL}{dt} + \frac{dD}{dt} + \frac{dN}{dt} \\ &= A - \omega(L + D + N) - \omega_1 D, \\ \frac{dM}{dt} &= A - \omega M - \omega_1 D, \end{aligned} \quad (5)$$

then,

$$\frac{dM}{dt} \leq A - \omega M,$$

integrate the equation above

$$M \leq M(0)e^{-\omega t} + \frac{A}{\omega}(1 - e^{-\omega t}), \quad (6)$$

We can get $\lim_{t \rightarrow \infty} M \leq \frac{A}{\omega}$. so \mathcal{U} , is a region that remains invariant under the dynamics of system (1). \square

Remark 3.1. Lemma (1) underscores the uniform persistence of system (1), signifying that the components of all solutions will eventually converge to a range bounded above and strictly away from zero, which aligns with biological plausibility.

4. Equilibrium points and threshold

The described system (1) features two equilibrium points that are non-negative.

(i) Propagation - free equilibrium, $E_0 = (\frac{A}{\omega}, 0, 0)$, when no propagation occurs [17, 18, 19], at which all the rumor propagation components are zeros.

$$\begin{cases} A - \frac{\beta LD}{1+\alpha D} - \omega L = 0, \\ \frac{\beta LD}{1+\alpha D} + \gamma N - (k + \omega + \omega_1)L = 0, \\ kD - (\gamma + \omega)N = 0. \end{cases} \quad (7)$$

when $D = 0, N = 0$, We can get $E_0 = (\frac{A}{\omega}, 0, 0)$.

(ii) Interior equilibrium $E^* = (L^*, D^*, N^*)$, when propagation persists in the system. We establish the existence of an equilibrium point E^* [19, 20] which is the focus of this section. Specifically, $E^* = (L^*, D^*, N^*)$ represents the positive solution to the equation derived from model system (1),

$$\begin{cases} A - \frac{\beta LD}{1 + \alpha D} - \omega L = 0, \\ \frac{\beta LD}{1 + \alpha D} + \gamma N - (k + \omega + \omega_1)L = 0, \\ kD - (\gamma + \omega)N = 0. \end{cases} \quad (8)$$

On solving above, we get

$$\begin{cases} L^* = \frac{\omega(k + \gamma + \omega + \omega_1) + \gamma\omega_1 + A\alpha(\omega + \gamma)}{(\omega + \gamma)(\beta + \alpha\omega)}, \\ D^* = \frac{(\omega + \gamma)N^*}{k}, \\ N^* = \frac{\beta L^*(\omega + \gamma) - \gamma k}{\alpha\gamma(\omega + \gamma)}. \end{cases} \quad (9)$$

Now we find the threshold, the number which the amount of secondary propagations. This is the mean value of propagations carried out by each individual disseminator during their entire propagation cycle, unhindered by any form of management measure [21, 22]. To solve the threshold, we use the next-generation matrix [23, 24]. Here in the system (1) D, N are the propagation contents and we decompose system (1) relating to the propagation contents as $F - V$, where Let $S = F(S) - V(S)$, where $S = (D, N)^T$, $F(S)$, is the propagation related term matrix, $V(S)$, is non propagation related term matrix. The propagation rumor class equations are the following:

$$\begin{aligned} \frac{dD}{dt} &= \frac{\beta LD}{1 + \alpha D} + \gamma N - (k + \omega + \omega_1)L, \\ \frac{dN}{dt} &= kD - (\gamma + \omega)N, \end{aligned} \quad (10)$$

Now, we have

$$F = \begin{bmatrix} \frac{\beta LD}{1 + \alpha D} \\ 0 \end{bmatrix}, V = \begin{bmatrix} -\gamma N + (k + \omega + \omega_1)D \\ -kD + (\gamma + \omega)N \end{bmatrix}. \quad (11)$$

Firstly, we identify the necessary Jacobi matrix.,

$$F_1(S) = \frac{\partial F}{\partial S} = \begin{bmatrix} \frac{\beta L}{(1 + \alpha D)^2} & 0 \\ 0 & 0 \end{bmatrix}. \quad (12)$$

The jacobi matrices $F_1(S)$, and $V_1(S)$ evaluated at $E_0 = (\frac{A}{\omega}, 0, 0)$, are provided as

$$F_1(S) = \frac{\partial F}{\partial S} = \begin{bmatrix} \frac{\beta A}{\omega} & 0 \\ 0 & 0 \end{bmatrix}, V_1(S) = \frac{\partial V}{\partial S} = \begin{bmatrix} \omega + \omega_1 + k & -\gamma \\ -k & \omega + \gamma \end{bmatrix}, \quad (13)$$

The threshold R_0 is the key metric that corresponds to the largest absolute value among the eigenvalues of the next generation matrix. $R_0 = \rho(F_1 V_1^-)$, signifying its pivotal role in quantifying the potential for disease spread.

$$V_1^-(S) = \begin{bmatrix} \frac{\omega + \gamma}{(\omega + \gamma)(\omega + \omega_1 + k) - k\gamma} & \frac{\gamma}{(\omega + \gamma)(\omega + \omega_1 + k) - k\gamma} \\ \frac{k}{(\omega + \gamma)(\omega + \omega_1 + k) - k\gamma} & \frac{k + \omega + \omega_1}{(\omega + \gamma)(\omega + \omega_1 + k) - k\gamma} \end{bmatrix}, \quad (14)$$

Then

$$\begin{aligned}
 D &= F_1 V_1^- \\
 &= \begin{bmatrix} \frac{\beta A}{\omega} & 0 \\ 0 & 0 \end{bmatrix} \begin{bmatrix} \frac{\omega + \gamma}{(\omega + \gamma)(\omega + \omega_1 + k) - k\gamma} & \frac{\gamma}{(\omega + \gamma)(\omega + \omega_1 + k) - k\gamma} \\ \frac{k}{(\omega + \gamma)(\omega + \omega_1 + k) - k\gamma} & \frac{k + \omega + \omega_1}{(\omega + \gamma)(\omega + \omega_1 + k) - k\gamma} \end{bmatrix}, \\
 &= \begin{bmatrix} \frac{\beta A(\omega + \gamma)}{\omega(\omega + \gamma)(\omega + \omega_1 + k) - \omega k \gamma} & \frac{\beta A \gamma}{\omega(\omega + \gamma)(\omega + \omega_1 + k) - \omega k \gamma} \\ 0 & 0 \end{bmatrix}
 \end{aligned} \tag{15}$$

Find the feature value

$$|\lambda E - D| = \begin{bmatrix} \lambda - \frac{\beta A(\omega + \gamma)}{\omega(\omega + \gamma)(\omega + \omega_1 + k) - \omega k \gamma} & -\frac{\beta A \gamma}{\omega(\omega + \gamma)(\omega + \omega_1 + k) - \omega k \gamma} \\ 0 & \lambda \end{bmatrix}, \tag{16}$$

work out;

$$\begin{aligned}
 \lambda^2 - \frac{\beta A(\omega + \gamma)}{\omega(\omega + \gamma)(\omega + \omega_1 + k) - \omega k \gamma} \lambda &= 0, \\
 \lambda_1 = 0, \lambda_2 &= \frac{\beta A(\omega + \gamma)}{\omega(\omega + \gamma)(\omega + \omega_1 + k) - \omega k \gamma},
 \end{aligned} \tag{17}$$

Thus, the threshold is obtained as follows:

$$R_0 = \frac{\beta A(\omega + \gamma)}{\omega(\omega + \gamma)(\omega + \omega_1 + k) - \omega k \gamma}. \tag{18}$$

We estimated the threshold R_0 , a measure of the average secondary spread caused by a single disseminator. The estimated high R_0 for each environment suggests that, without intervention, outbreaks of rumor could potentially lead to substantial final propagation. Therefore, once the propagation of rumor sentiment is detected in a given environment, urgent intervention is crucial.

5. Stability of the model

In this section, we explore the stability characteristics of the model system (1) at both the Propagation-Free Equilibrium (PFE) and the Interior equilibrium points. We can get a Dissemination-free equilibrium (PFE) $E_0 = (\frac{A}{\omega}, 0, 0)$, when no propagation occurs. A Interior equilibrium $E^* = (L^*, D^*, N^*)$, when propagation persists in the system.

5.1. local stability

Initially, we identify the necessary Jacobian matrix and ascertain the sign of its eigenvalues. According to the principles of differential equations, should all eigenvalues of the Jacobian matrix possess negative real components, it follows that E^* is locally asymptotically stable. We reproduce a definition $X = L - L^*$, $Y = D - D^*$, $Z = N - N^*$, the linearized system reads as

$$\begin{cases} \frac{dX}{dt} = -\frac{\beta XY}{1 + \alpha Y} - \omega X = f_1 \\ \frac{dY}{dt} = \frac{\beta XY}{1 + \alpha Y} + \gamma Z - (k + \omega + \omega_1)Y = f_2 \\ \frac{dZ}{dt} = kY - \omega Z - \gamma Z = f_3. \end{cases} \tag{19}$$

The Jacobian matrix is then given by

$$J = \begin{bmatrix} \frac{df_1}{dL} & \frac{df_1}{dD} & \frac{df_1}{dN} \\ \frac{df_2}{dL} & \frac{df_2}{dD} & \frac{df_2}{dN} \\ \frac{df_3}{dL} & \frac{df_3}{dD} & \frac{df_3}{dN} \end{bmatrix},$$

Theorem 5.1. *Propagation-free equilibrium E_0 of the model is locally asymptotically stable if $R_0 < 1$, and it is unstable if $R_0 > 1$.*

We calculate the jacobian matrix J_0 of the system around the given Propagation-free equilibrium (PFE) $E_0 = (\frac{A}{\omega}, 0, 0)$, when no infection occurs, and it is provided by

$$J_0 = \begin{bmatrix} -\omega & \frac{-\beta A}{\omega} & 0 \\ 0 & \frac{\beta A}{\omega} - (k + \omega + \omega_1) & \gamma \\ 0 & k & -(\omega + \gamma) \end{bmatrix},$$

We calculate the jacobian matrix J_0

$$|\lambda E - J_0| = \begin{bmatrix} \lambda + \omega & \frac{\beta A}{\omega} & 0 \\ 0 & \lambda - \frac{\beta A}{\omega} + (k + \omega + \omega_1) & -\gamma \\ 0 & -k & \lambda + (\omega + \gamma) \end{bmatrix},$$

After some computations, the characteristic equation is

$$C(\lambda) = \lambda^3 + A_1\lambda^2 + A_2\lambda + A_3 = 0 \quad (20)$$

where

$$\begin{cases} A_1 = \omega + \omega_1 + \gamma + k - \frac{\beta A}{\omega}, \\ A_2 = (3\omega + 2\omega + 2\omega_1 + \gamma)\omega - 2\beta A - (k + \omega + \omega_1 - \frac{\beta A}{\omega})\gamma \\ A_3 = \omega(\gamma + k + \omega_1)(\gamma + \omega) - k\omega\gamma. \end{cases}$$

According to Vieta's theorem:

$$\begin{aligned} \lambda_1 + \lambda_2 + \lambda_3 &= -(\omega + \omega_1 + \gamma + k) + \frac{\beta A}{\omega}, \\ \lambda_1\lambda_2 + \lambda_1\lambda_3 + \lambda_2\lambda_3 &= (3\omega + 2\omega + 2\omega_1 + \gamma)\omega - 2\beta A - (k + \omega + \omega_1 - \frac{\beta A}{\omega})\gamma, \\ \lambda_1\lambda_2\lambda_3 &= \omega(\gamma + k + \omega_1)(\gamma + \omega) - k\omega\gamma. \end{aligned}$$

Consider $R_0 < 1$, and Propagation-free equilibrium point E_0 , the characteristic roots, λ_1 , λ_2 and λ_3 are negative. The roots of the characteristic equation have a negative real part if and only if Routh-Hurwitz criterion that symbol E_0 is locally asymptotically stable. Then, E_0 is locally asymptotically stable since the corresponding Routh-Hurwitz criteria is satisfied, given by $A_1 > 0$, $A_3 > 0$, $A_1A_2 > A_3$. When $R_0 > 1$, the three characteristic roots are not all negative, and the Hurwitz stability criterion that Dissemination-free equilibrium point E_0 is unstable in this case.

Theorem 5.2. *The Interior equilibrium is locally asymptotically stable if and only if $R_0 > 1$.*

We find a Jacobian system matrix around the interior equilibrium $E^* = (L(t)^*, D(t)^*, N(t)^*)$ from system (1), It is given by J_*

$$J_* = \begin{bmatrix} \frac{-\beta D^*}{1+\alpha D^*} - \omega & \frac{-\beta D^*}{(1+\alpha D^*)^2} & 0 \\ \frac{\beta D^*}{1+\alpha D^*} & \frac{\beta L^*}{(1+\alpha D^*)^2} - (K + \omega + \omega_1) & \gamma \\ 0 & k & -(\omega + \gamma) \end{bmatrix},$$

We calculate the jacobian matrix J_*

$$|\lambda E - J_*| = \begin{bmatrix} \lambda + \frac{\beta D^*}{1+\alpha D^*} + \omega & \frac{\beta D^*}{(1+\alpha D^*)^2} & 0 \\ \frac{-\beta D^*}{1+\alpha D^*} & \lambda - \frac{\beta L^*}{(1+\alpha D^*)^2} + (k + \omega + \omega_1) & -\gamma \\ 0 & -k & \lambda + (\omega + \gamma) \end{bmatrix},$$

After some computations, the characteristic equation is

$$g(\lambda) = \lambda^3 + b_1\lambda^2 + b_2\lambda + b_3 = 0 \quad (21)$$

where

$$\left\{ \begin{array}{l} b_1 = 3\omega + \omega_1 + k + \gamma + \frac{\beta D^*}{1 + \alpha D^*} - \frac{\beta L^*}{(1 + \alpha D^*)^2}, \\ b_2 = (k + \omega + \omega_1)(2\omega + \gamma) + \omega(\omega + \gamma) - k\gamma + \frac{2\beta^2 L^* D^*}{(1 + \alpha D^*)^3} \\ \quad + \frac{\beta L^* \gamma}{1 + \alpha D^{*2}} + \frac{\beta D^*}{1 + \alpha D^*}(2\omega + \omega_1 + k + \gamma), \\ b_3 = \omega(k + \omega + \omega_1)(\omega + \gamma) - k\omega\gamma + \frac{2\beta^2 L^* D^*}{(1 + \alpha D^*)^3}(\omega + \gamma) \\ \quad - \frac{\beta L^*}{1 + \alpha D^{*2}}\omega(\omega + \gamma) + \frac{\beta D^*(\omega + \omega_1 + k)(\omega + \gamma) - k\gamma}{1 + \alpha D^*}. \end{array} \right.$$

We can get,

$$\begin{aligned} \lambda_4 + \lambda_5 + \lambda_6 &= -(3\omega + \omega_1 + k + \gamma) - \frac{\beta D^*}{1 + \alpha D^*} + \frac{\beta L^*}{(1 + \alpha D^*)^2}, \\ \lambda_4\lambda_5 + \lambda_4\lambda_6 + \lambda_5\lambda_6 &= (k + \omega + \omega_1)(2\omega + \gamma) + \omega(\omega + \gamma) - k\gamma + \frac{2\beta^2 L^* D^*}{(1 + \alpha D^*)^3} \\ &\quad + \frac{\beta L^* \gamma}{1 + \alpha D^{*2}} + \frac{\beta D^*}{1 + \alpha D^*}(2\omega + \omega_1 + k + \gamma), \\ \lambda_4\lambda_5\lambda_6 &= -\omega(k + \omega + \omega_1)(\omega + \gamma) + k\omega\gamma - \frac{2\beta^2 L^* D^*}{(1 + \alpha D^*)^3}(\omega + \gamma) + \frac{\beta L^*}{1 + \alpha D^{*2}}\omega(\omega + \gamma) \\ &\quad - \frac{\beta D^*(\omega + \omega_1 + k)(\omega + \gamma) - k\gamma}{1 + \alpha D^*}. \end{aligned}$$

Consider $R_0 > 1$, and Interior equilibrium point E^* , the characteristic roots, λ_4 , λ_5 and λ_6 , are negative. According to Hurwitz stability criterion, propagation equilibrium point E^* is locally stable.

5.2. Global stability of the interior equilibrium

Consider the Lyapunov function:

$$\begin{aligned} H &= [(L - L^*) + (D - D^*) + (N - N^*)]^2, \\ H' &= 2[(L - L^*) + (D - D^*) + (N - N^*)][L' + D' + N'] \\ &= 2[(L - L^*) + (D - D^*) + (N - N^*)][A - \omega L - \omega D - \omega N - \omega_1 D], \end{aligned}$$

Because we know $A - \omega L^* - \omega D^* - \omega N^* - \omega_1 D^* = 0$, in other words $A = \omega L^* + \omega D^* + \omega N^* + \omega_1 D^*$, we can get

$$\begin{aligned} H' &= 2[(L - L^*) + (D - D^*) + (N - N^*)][\omega L^* + \omega D^* + \omega N^* + \omega_1 D^* - \omega L^* \\ &\quad - \omega D^* - \omega N^* - \omega_1 D^*], \\ &= 2[(L - L^*) + (D - D^*) + (N - N^*)][\omega(L^* - L) + \omega(D^* - D) + \omega(N^* - N) \\ &\quad + \omega_1(D^* - D)] \\ &= -2\omega[(L - L^*) + (D - D^*) + (N - N^*)][\omega + \omega_1(D - D^*)] \leq 0. \end{aligned}$$

Consequently, the internal equilibrium $E^*(L^*, D^*, N^*)$ of system (1) is shown to be globally asymptotically stable, in accordance with LaSalle's Invariance Principle.

6. Numerical simulation

Existing literature lacks a definitive and consistent standard for the parameter ranges within the model, typically only requiring them to be positive. Drawing on parameter values from related works and considering stability constraints, we assign parameter values for our numerical simulations. These simulations validate the logical coherence of our theoretical findings. We then carry out numerical simulations using these parameter values to confirm the accuracy of our earlier inferences. In conclusion, we conduct a sensitivity analysis on the model to investigate the relationship between the basic reproductive number and the various parameters.

In this section, we delve into the influence of diverse parameters on the threshold value. Through Matlab simulations, we gain a comprehensive understanding of which parameter exerts the most significant influence on L, D, N and C . We choose $\beta, \omega, \omega_1, k, \gamma, \alpha, A$. The influence of $A, k, \omega, \beta, \gamma$ and ω_1 on L, D, N and C is analyzed by assigning values.

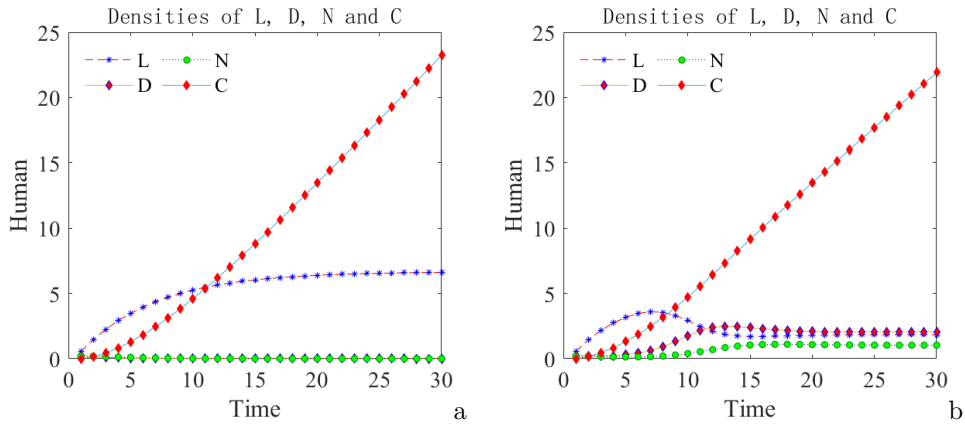


FIGURE 2. The densities of L, D, N , and C under parameter β .

Fig. 2(a) (b), β is propagation rate from population L to population D , and shows that as β increases, D increase and L decrease; β has the greatest influence on D and L ; the speed of D increase is from fast to slow; the speed of N and C increase is from fast to slow; D increases first and then becomes stable; and L decreases first and then becomes stable.

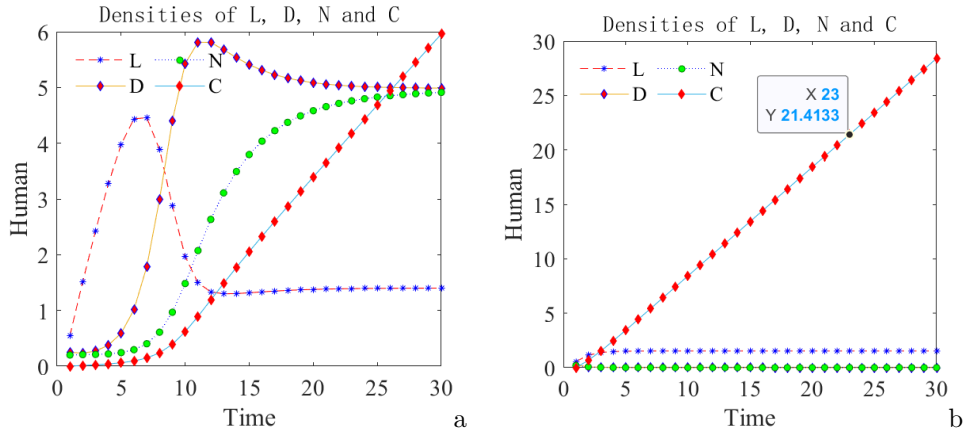
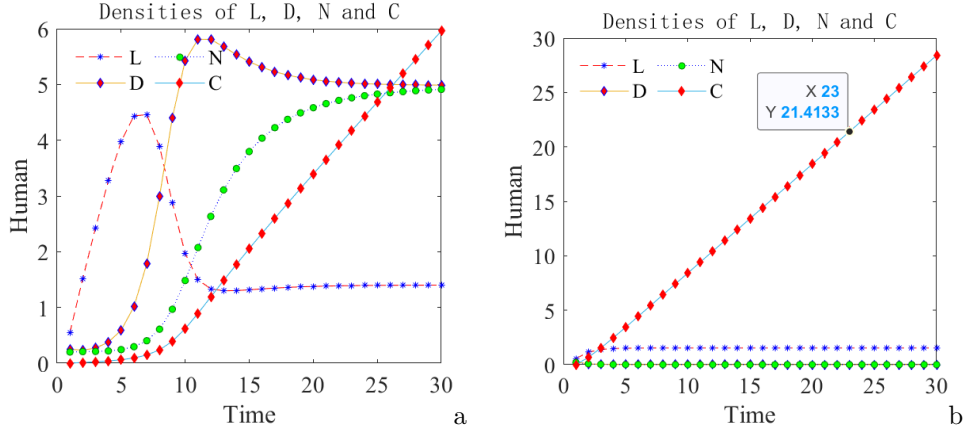
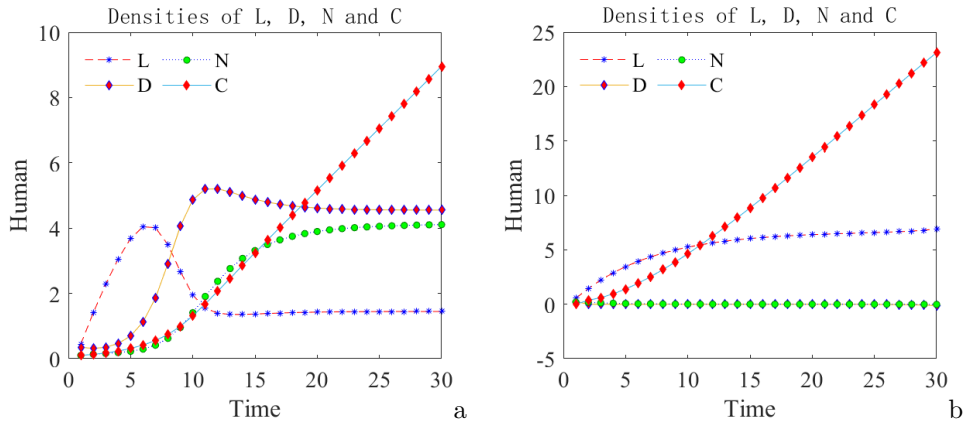
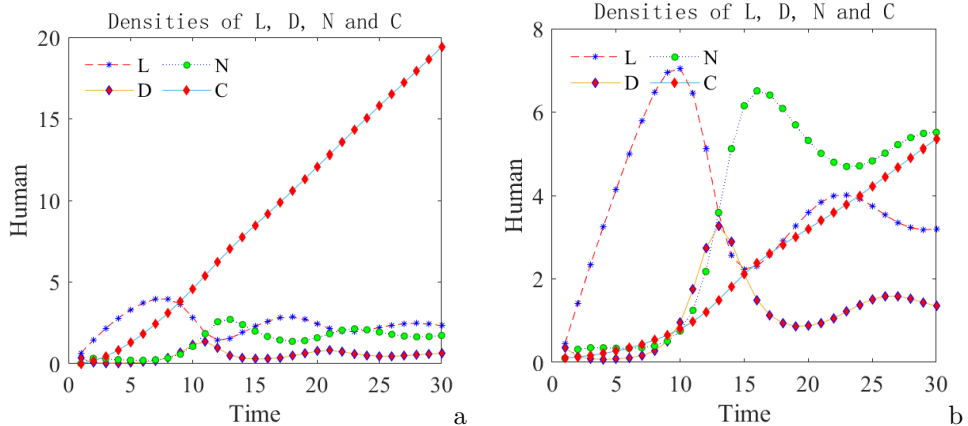
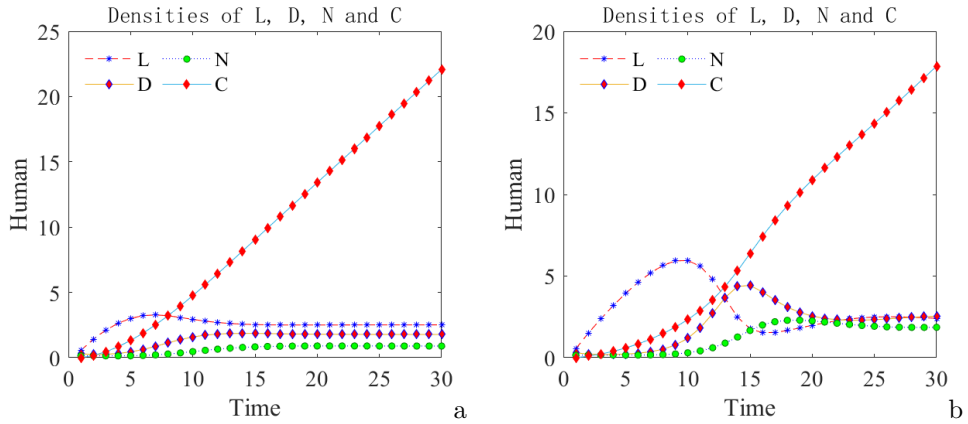
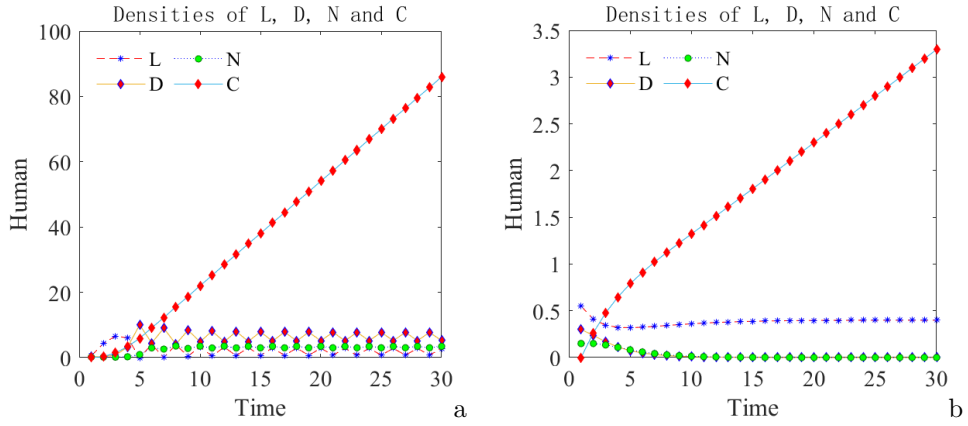


FIGURE 3. The densities of L, D, N , and C under parameter ω .

FIGURE 4. The densities of L, D, N, and C under parameter ω_1 .FIGURE 5. The densities of L, D, N, and C under parameter k .FIGURE 6. The densities of L, D, N, and C under parameter γ .

In Fig. 3(a)(b), ω represents the outflow rate from population L, D, and N to population C, and shows that when ω increases, C increase and L, D and N decrease. The curves

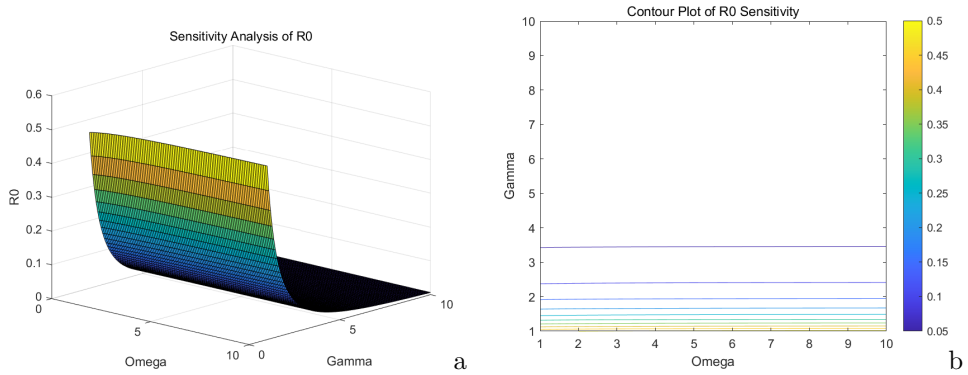
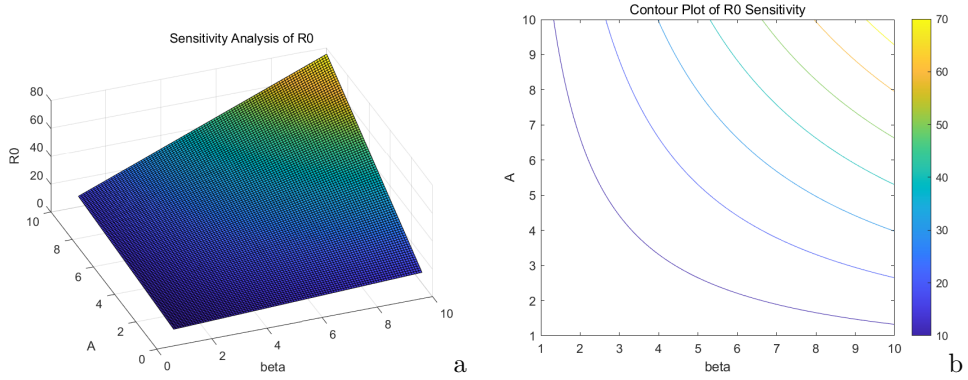
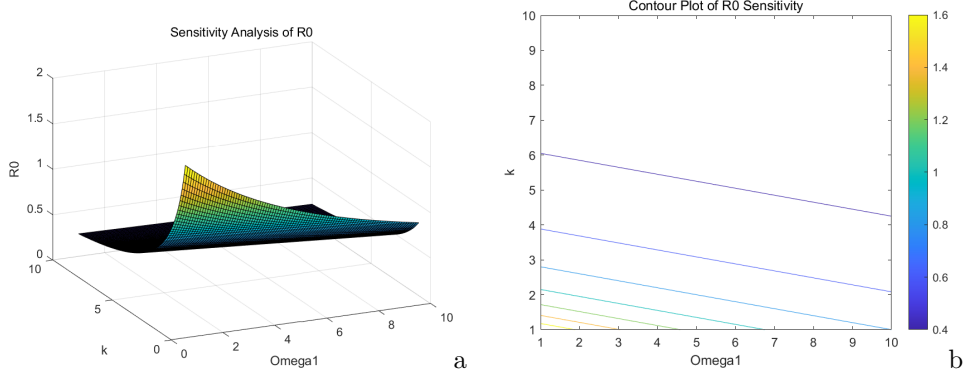
FIGURE 7. The densities of L, D, N, and C under parameter α .FIGURE 8. The densities of L, D, N, and C under parameter A .

of L, D and N flatten out. In Fig. 4(a) (b), ω_1 is the leave the environment's dissemination rate from population D to population C; when ω_1 increases, C increase; ω_1 has the greatest influence on C and as ω_1 increases, the number of C increase.

In Fig. 5(a) (b), k is the termination rate of this propagation from population D to population N, and shows that when k increases, N increase and D decrease. The curves of L and D flatten out. In Fig. 6(a) (b), γ represents the recurrence rate of rumor propagation forgetting rate from population N to population D; when γ increases, D increase; the number of γ increases, N decrease.

In Fig. 7(a) (b), The parameter α exerts an inhibitory influence on the individuals responsible for rumor propagation, demonstrating that as α rises, L increases while D decreases. Additionally, α has a negligible impact on N and C, with the corresponding curves exhibiting a tendency to remain relatively flat. Considering Fig. 8(a)(b), parameter A has a greater impact on the latent disseminators, therefore, latent disseminators who are more likely to believe and spread them.

The sensitivity analysis of ω and γ on R_0 is shown in Fig. 9(a) (b). The sensitivity analysis of β and A on R_0 is shown in Fig. 10(a) (b). The sensitivity analysis of ω_1 and k on R_0 is shown in Fig. 11(a) (b). When both variables decline, it suggests that implementing rumor prevention strategies and establishing a set of punitive measures can effectively control the spread of rumors.

FIGURE 9. Sensitivity analysis of ω and γ on R_0 .FIGURE 10. Sensitivity analysis of β and A on R_0 .FIGURE 11. Sensitivity analysis of ω_1 and k on R_0 .

7. Conclusion

The dynamics of rumor refers to the study of the dynamic states of mathematical models that illustrate the evolution of rumor. As a powerful tool, it aids in analyzing key elements of rumor, providing theoretical and quantitative foundations for the development of preventive . Recently, the prevention of rumor have become critical issues, closely related

to human welfare and daily life. Therefore, researching the propagation dynamics of rumor is of significant importance.

In this paper, we categorize the population within the rumor environment into four groups: latent disseminators, disseminators, non-disseminators, and leavers. We then establish an *LDN* model that incorporates factors such as the rumor channelization coefficient, population inflow and outflow rates. Acknowledging the limitations of preventive measures, we consider the propagation rates to be of a saturated type. We derive the threshold of the model, which is crucial in assessing the stability of propagation. By identifying the model's equilibrium point, we analyze its relationship with the crisis's development trend and derive the threshold R_0 . Subsequently, we examine the factors influencing R_0 through numerical experiments. Finally, we provide a detailed analysis of how these factors impact the development trend of rumor. When $R_0 < 1$, the propagation-free equilibrium is stable within a specific range, and propagation exhibits a downward trend until it ultimately dissipates. Based on these findings, we offer policy recommendations.

8. Acknowledge

This research received partial funding from the National Social Science Fund Project, which focuses on the study of the co-creation of ecosystem value for green brands in the characteristic agricultural sector of Northwest China under the twin carbon targets (Project Number 23BMZ062). The North Minzu University of China (Project Number 2022ZLGT-TYS12). Additional support was provided by the Key Projects of North Minzu University (Project Number ZDZX201805), the Governance and Social Management Research Center of Northwest Ethnic Regions, the First-Class Disciplines Foundation of Ningxia (Project Number NXYLXK2017B09), the Ningxia Youth Talent Support Program (2021), and the Leading Talent Support Program of North Minzu University.

REFERENCES

- [1] Bhowmik, Sima, and Jolene Fisher. "Framing the Israel-Palestine conflict 2021: Investigation of CNN's coverage from a peace journalism perspective." *Media, Culture & Society* 2023 vol. 45, no. 5 pp.1019-1035.
- [2] Gruen, George E. "Contribution of water imports to Israeli-Palestinian-Jordanian peace." *Studies in Environmental Science*. Vol. 58. Elsevier, 1994. pp. 273-288.
- [3] Wang J, Zhang X, Liu W, et. "Spatiotemporal pattern evolution and influencing factors of online public opinion—Evidence from the early-stage of COVID-19 in China." *Heliyon* 2023 9. 9.
- [4] Xu Z, Zhan B, Wang S. "Public opinion risk on major emergencies: A textual analysis." *Procedia Computer Science*, 2023, pp. 833-838.
- [5] Mohd Suhairi Md Suhaimin, Mohd Hanafi Ahmad Hijazi, Ervin Gubin Moung, Puteri Nor Ellyza Nohuddin, Stephanie Chua, Frans Coenen. "Social media sentiment analysis and opinion mining in public security: Taxonomy, trend analysis, issues and future directions Journal of King Saud University." *Computer and Information Sciences*, 2023, vol. 35, no. 9, pp.1319-1578.
- [6] Bingtao Wan, Peng Wu, Chai Kiat Yeo, Gang Li, "Emotion-cognitive reasoning integrated BERT for sentiment analysis of online public opinions on emergencies." *Information Processing & Management*, 2024, vol. 61, no. 2, pp.0306-4573.
- [7] Jinghua Zhao, Huihong He, Xiaohua Zhao, Jie Lin, "Modeling and simulation of microblog-based public health emergency-associated public opinion communication." *Information Processing & Management*, 2022, vol. 59, no. 2, pp. 0306-4573.
- [8] Y. Wang and W. Cai, "Epidemic spreading model based on social active degree in social networks." *CHINA COMMUNICATIONS*, 2015, vol. 12, pp. 101-108.

[9] Qi S, Jinli G, School B, " Spreading model and simulation analysis of Internet public opinion in hyper-networks." *Application Research of Computers*, 2017.

[10] K. Kandhway and J. Kuri, " Accelerating information diffusion in social networks under the Susceptible-Infected-Susceptible epidemic model." *International Conference on Advances in Computing, Communications and Informatics (ICACCI)*, 2014, pp.1515-1519.

[11] Shiyue Li, Zixuan Liu, Yanling Li, " Temporal and spatial evolution of online public sentiment on emergencies." *Information Processing & Management*, 2020, vol. 57, no. 2, pp.0306-4573.

[12] Xueyong Zhou, Jingan Cui, " Analysis of stability and bifurcation for an SEIR epidemic model with saturated recovery rate." *Communications in Nonlinear Science and Numerical Simulation*, 2011, vol. 16, no. 11, pp. 4438-4450.

[13] Kumar, A, " Nilam Dynamical Model of Epidemic Along with Time Delay; Holling Type II Incidence Rate and Monod-Haldane Type Treatment Rate." *Differ Equ Dyn Syst*, 2019, vol. 27, pp. 299-312

[14] Li Dan, " Research on Crisis Communication Mechanism Based on Dynamic Model." *Northern University for Nationalities*, 2020.

[15] Preeti Dubey, Balram Dubey, Uma S. Dubey, " An SIR Model with Nonlinear Incidence Rate and Holling Type III Treatment Rate." *Applied Analysis in Biological and Physical Sciences*, 2016, pp. 186.

[16] Arjun Kumar, Ashvini Gupta, Uma S. Dubey, Balram Dubey, " Stability and bifurcation analysis of an infectious disease model with different optimal control strategies." *Mathematics and Computers in Simulation*, 2023, vol. 213, pp. 78-114.

[17] Yuhang Hu, Hao Liu, Jian Zhao, Liangping Tu, " Dynamic analysis of dissemination model of innovation ability of enterprise R & D personnel." *Physica A: Statistical Mechanics and its Applications*, 2019, pp. 0378-4371.

[18] Anastasios Evgenidis, Athanasios Tsagkanos, Costas Siriopoulos, "Towards an asymmetric long run equilibrium between stock market uncertainty and the yield spread. A threshold vector error correction approach." *Research in International Business and Finance*, 2017, vol. 39, pp. 267-279.

[19] Nasir H, " A time-delay model of diabetic population: Dynamics analysis, sensitivity, and optimal control." *Physica Scripta*, 2021, vol. 96, no. 11, pp. 23.

[20] Ryosuke Omori, Teruyoshi Hagino, Puttirungroj Pattama, Kenichi Ozaki, Ikuo Hirono, " Estimating the basic reproduction number and final epidemic size of white spot syndrome virus outbreak in *Penaeus japonicus* in aquaculture ponds." *Aquaculture*, 2024, pp. 0044-8486.

[21] Yi Wang, Junling Ma, Jinde Cao, " Basic reproduction number for the SIR epidemic in degree correlated networks." *Physica D: Nonlinear Phenomena*, 2022, vol. 433, pp. 0167-2789.

[22] Jufren Zakayo Ndendya, Leonce Leandry, Andrea M. Kipingu, "A next-generation matrix approach using Routh-Hurwitz criterion and quadratic Lyapunov function for modeling animal rabies with infective immigrants." *Healthcare Analytics*, 2023, vol. 4, pp. 2772-4425.

[23] Xiaohua Zhang, Xin Wang, Wenling Jiao, Yitao Liu, Jianyong Yu, Bin Ding, " Evolution from microfibers to nanofibers toward next-generation ceramic matrix composites: A review." *Journal of the European Ceramic Society*, 2023, vol. 43, no. 4, pp. 1255-1269.

[24] Shouyuan Jiang, Steven G. Wise, Jason C. Kovacic, Jelena Rnjak-Kovacina, Megan S. Lord, " Biomaterials containing extracellular matrix molecules as biomimetic next-generation vascular grafts." *Trends in Biotechnology*, 2024, vol. 42, no. 3, pp. 369-381.